



Simulation for generation of 15 fs laser pulses by Raman backscatter in plasmas

Min Sup Hur, Jaehoon Kim, Devki N. Gupta, Hyo Jae Jang, and Hyoyong Suk

Citation: [Applied Physics Letters](#) **91**, 101501 (2007); doi: 10.1063/1.2779926

View online: <http://dx.doi.org/10.1063/1.2779926>

View Table of Contents: <http://scitation.aip.org/content/aip/journal/apl/91/10?ver=pdfcov>

Published by the [AIP Publishing](#)

Articles you may be interested in

[Kinetic simulations of stimulated Raman backscattering and related processes for the shock-ignition approach to inertial confinement fusion](#)

[Phys. Plasmas](#) **18**, 092701 (2011); 10.1063/1.3630937

[Envelope-kinetic analysis of the electron kinetic effects on Raman backscatter and Raman backward laser amplification](#)

[Phys. Plasmas](#) **14**, 033104 (2007); 10.1063/1.2646493

[Effects of the frequency detuning in Raman backscattering of infinitely long laser pulses in plasmas](#)

[Phys. Plasmas](#) **13**, 073103 (2006); 10.1063/1.2222327

[Manipulating ultrashort intense laser pulses by plasma Bragg gratings](#)

[Phys. Plasmas](#) **12**, 113103 (2005); 10.1063/1.2126587

[Slowly varying envelope kinetic simulations of pulse amplification by Raman backscattering](#)

[Phys. Plasmas](#) **11**, 5204 (2004); 10.1063/1.1796351

Not all AFMs are created equal
Asylum Research Cypher™ AFMs
There's no other AFM like Cypher

www.AsylumResearch.com/NoOtherAFMLikeIt


The Business of Science®

The advertisement features a blue background with a film strip on the left side. The text is in white and orange. The Oxford Instruments logo is in the bottom right corner.

Simulation for generation of 15 fs laser pulses by Raman backscatter in plasmas

Min Sup Hur, Jaehoon Kim, Devki N. Gupta, Hyo Jae Jang, and Hyyong Suk^{a)}

Center for Advanced Accelerators, Korea Electrotechnology Research Institute, Changwon, Kyongnam 641-120, Korea

(Received 28 June 2007; accepted 14 August 2007; published online 5 September 2007)

Pulse compression using the Raman backscatter (RBS) in plasmas was numerically investigated for the strong kinetic regime. It was found that shortening of a seed pulse is more effective when the interaction length is smaller, which is contradictory to the general expectation. In a representative case, compression of up to 14 fs could be obtained from the RBS interaction length less than 0.1 mm. Behavior of the Raman amplification system for such a short interaction distance was not addressed before. Estimation with realistic parameters indicates that the output power can reach tens of terawatts. © 2007 American Institute of Physics. [DOI: 10.1063/1.2779926]

Owing to the chirped-pulse-amplification (CPA) technique, the high power laser technology has been improved quite rapidly. However, applications of ultraintense and ultrashort laser pulses such as the laser wakefield acceleration¹ (LWFA) and the fast ignition in the inertial confinement fusion² require even more enhanced power and, simultaneously, much shorter pulse duration. The minimum pulse duration of tens of terawatt lasers currently available from the CPA technique is known to be larger than 25 fs. Technical difficulty with regard to the pulse shortening below 25 fs in the CPA is that complicated bandwidth filtering methods are needed to generate short laser pulses due to the gain narrowing effect in the amplifier. On the other hand, generation of sub-10 fs pulses has been reported in several contexts,^{3,4} but the power of the output pulse for all those cases is much below 1 TW. Thus, the power enhancement and pulse shortening are apparently not so compatible with each other.

One of the promising methods to obtain the ultraintense power and ultrashort pulse duration simultaneously is utilizing the Raman backscatter (RBS) of a pump laser in a plasma.⁵⁻⁹ In the RBS scheme, the pump laser energy is transferred to the counterpropagating seed laser pulse via RBS process, leading to the compression and amplification of the seed pulse. From the RBS scheme, though people expect theoretically much stronger and shorter pulse generation to be possible, just 26 fs in the superradiant regime⁷ and 150 fs in the Raman regime⁸ with gigawatt powers have been achieved in the experiments. From kinetic simulations, a sub-5 fs pulse in the super-radiant regime was obtained by Shvets *et al.*⁹ In that case, however, initial duration of the pulse was very short already (about 10 fs). The major technical difficulty of all those cases is that the laser pulse is required to propagate a millimeter-order long plasma, which is not easy to put under control of the fluctuation and instabilities.

In this letter, we investigate numerically the properties of the RBS scheme for *extremely short* interaction between the seed and intense Gaussian pump pulses. It has been indicated from the fluid theories and simulations that the seed pulse gains higher peak intensity and more pulse shortening as the

interaction length increases. However, it was found from our kinetic studies that the pulse shortening often shows the opposite behavior: pulse duration becomes smaller for shorter interaction in the strong kinetic regime. Motivated by such observation, we investigated the cases where the pump pulse duration is significantly shorter than that of the previous works. One of the most interesting results from our numerical studies is the compression of the initial 30 fs seed pulse down to 16 fs, as the details will be described later. The pump length for that representative case was only 970 fs and the interaction length was just 0.15 mm. When the pump duration was reduced by half, even more shortening of the seed pulse was obtained.

Other than the good efficiency in the pulse shortening, using a short pump pulse has many technical advantages. To be fitted to the several hundred femtosecond pump duration, the longitudinal length of the plasma needs only to be some fractions of a millimeter. Such a small-size plasma is less prone to fluctuation than the millimeter-order long plasma. Another virtue of minimizing the interaction length is that various undesirable laser-plasma instabilities can be avoided.

For the kinetic simulation studies, the one-dimensional averaged particle-in-cell (APIC) code⁶ was used. In the APIC, the longitudinal motion of the plasma is treated fully kinetically by the PIC method, and the evolution of the lasers is traced by their envelopes. The envelope-kinetic equations of the laser envelopes^{6,9} are

$$\frac{\partial}{\partial t} a_1 + c \frac{\partial}{\partial z} a_1 = - \frac{\omega_p}{2} f^* a_2, \quad (1a)$$

$$\frac{\partial}{\partial t} a_2 - c \frac{\partial}{\partial z} a_2 = \frac{\omega_p}{2} f a_1, \quad (1b)$$

$$f = -i \frac{\omega_p}{\omega} \langle e^{-i\phi_j} \rangle, \quad (1c)$$

where $a_{1,2}$ represent the envelopes of the normalized vector potential of the seed and pump, respectively, and ω_p is the plasma frequency defined by $\sqrt{e^2 n_0 / m \epsilon_0}$. Here, e and m are the charge and mass of an electron, respectively, n_0 is the plasma density, and ϵ_0 is the electrical permittivity of free space. The plasma wave envelope is denoted by f and ω is

^{a)}Electronic address: hysuk@keri.re.kr

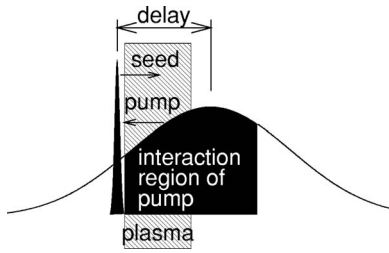


FIG. 1. Position of the laser pulses and the plasma at $t=0$. The rectangle filled with oblique lines represents the plasma. The seed and pump pulses propagate to the right and the left, respectively. The dark region inside the pump profile indicates the interacting part with the seed and the plasma, which is two times longer than the plasma. The delay of the pump is defined by the temporal distance of the peak of the pump pulse measured from the peak of the seed.

the average of the seed and pump frequencies ω_1 and ω_2 . The angular bracket represents an ensemble average of the simulation particles over a beat wavelength of the two laser pulses. The ponderomotive phase ϕ_j of the j th particle is defined by the beat of the two lasers, $-(k_1+k_2)z_j - (\omega_2 - \omega_1)t$. In deriving Eq. (1), the spatiotemporally fast oscillating terms $\sim e^{\pm ik_{1,2}z - i\omega_{1,2}t}$ were averaged out. It is assumed in Eq. (1) that $\omega_p \ll \omega_{1,2}$, which is satisfied for all the simulations presented in this letter. The slow longitudinal motion of the plasma is driven by the ponderomotive force and the self-generated electrostatic force. The ponderomotive driving arises predominantly from the beat of the two counterpropagating lasers. The electrostatic field is calculated by the conventional PIC method.

Figure 1 represents the arrangement of the seed and pump pulses at $t=0$. The seed pulse is located in such a way that its front cutoff at 2σ (for $a_1 \sim e^{-t^2/\sigma^2}$) touches the vacuum-plasma boundary. For the plasma, we used a steplike density profile, i.e., $n=0$ for $z < 0$ or $z > L$ and $n=n_0$ for $0 \leq z \leq L$, where L is the plasma length. The interaction region in the pump pulse is approximately two times the plasma length. The delay of the pump pulse is defined by the temporal distance of the peak of the pump measured from the peak of the seed. The effects of the pump delay will be discussed later.

A representative case of the pulse compression is presented in Fig. 2. The seed pulse started with 31.4 fs in full

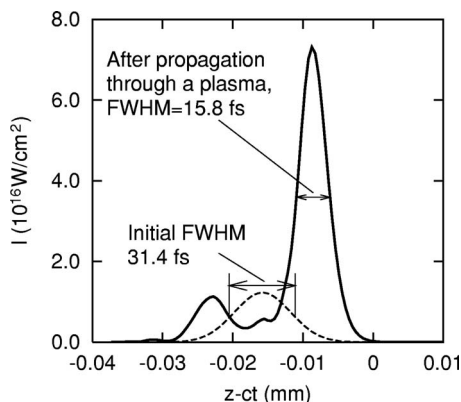


FIG. 2. Representative simulation result, where 15.8 fs pulse was generated. The amplified seed (solid line) is moving to the right. The dashed line represents the seed pulse at $t=0$ and the propagation distance of the compressed seed is 0.145 mm. The normalized amplitudes of the seed and pump at $t=0$ are $a_1=0.1$ and $a_2=0.07$, respectively. The plasma density and temperature are $n_0=2.8 \times 10^{19} \text{ cm}^{-3}$ and 10 eV, respectively.

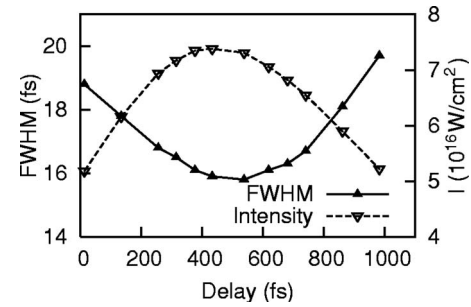


FIG. 3. (a) Pulse duration and (b) intensity as a function of the initial delay between the seed and pump pulses. Delay of 538 fs corresponds to the strongest interaction, i.e., interaction with the full width half maximum of the pump.

width half maximum (FWHM) and $I_1=1.2 \times 10^{16} \text{ W/cm}^2$. The initial intensity I_1 of the seed corresponds to $a_1=0.1$ for $\lambda_1=1.05 \mu\text{m}$. The length of the plasma and the density were $L=0.145 \text{ mm}$ and $n_0=2.8 \times 10^{19} \text{ cm}^{-3}$, respectively. The plasma temperature was taken to be 10 eV. The pulse duration of the pump pulse was 970 fs (FWHM), and the amplitude was $a_2=0.07$, corresponding to $I_2=8.2 \times 10^{15} \text{ W/cm}^2$ for $\lambda_2=0.9 \mu\text{m}$. The seed and pump pulses were arranged in order that the seed could interact with the strongest part of the pump pulse, i.e., the FWHM region. The delay (as defined in Fig. 1) to meet such condition is 538 fs. After propagation through the plasma, the pulse duration and the intensity were measured to be 15.8 fs and $7.3 \times 10^{16} \text{ W/cm}^2$, respectively. In this case, the amplification of the intensity is a factor of 6.

The one-dimensional results do not give an exact information about the power, since the power depends on the transverse spot size. However, some possible values can be estimated by reasonably assuming certain numbers for the spot size. As described in Ref. 5, the original RBS scheme indicates that a weak (but still strong compared to other method such as CPA) and unfocused seed laser goes through the Raman or the superradiant interaction. Then the amplified pulse is focused into a high intensity. In that sense, the unfocused radius of the amplified seed in Fig. 2 can be taken as, for instance, 200 μm , which leads to a 45 TW, 15.8 fs laser pulse. The required initial power of the seed is 7.5 TW. The transverse size of the plasma has to match just the seed spot, which can be satisfied by less than 0.8 mm. The small size of the plasma, $0.8 \times 0.145 \text{ mm}$, is quite desirable, since such a small plasma can be put under control of the density fluctuation more easily than the millimeter-order plasmas, and the refraction and instabilities of the pump pulse can be minimized.

It was found that the final pulse intensity and duration are quite robust to the variation in the seed-pump delay. Figure 3 exhibits the pulse duration of the seed [Fig. 3(a)] and its intensity [Fig. 3(b)] as functions of the delay. As can be expected, the maximum (minimum) amplification (duration) is obtained when the seed interacts with the strongest region of the pump (the case of Fig. 2). The variation in the pulse duration and the intensity over the delay varying from 300 to 700 fs are just 5% and 7%, respectively. Such a huge margin in the delay for stable operation enables the RBS scheme in short plasmas be realized even more easily at the laboratories.

The effect of plasma edge was found to be very minor. When the simulation was done with identical parameters but

TABLE I. Peak intensity (I_1) and pulse duration (τ_1) of the seed pulse after compression. The parameters a_2 and τ_2 are the input values of the normalized vector potential and the pulse duration of the pump, respectively. The parameter L indicates the length of the plasma. The initial parameters of the seed pulse are constant for all cases.

a_2	τ_2 (fs)	L (mm)	I_1 (W/cm ²)	τ_1 (fs)
0.07 ^a	970	0.145	7.3×10^{16}	15.8
0.099	485	0.0725	5.3×10^{16}	14.0
0.07	485	0.0725	4.22×10^{16}	15.8
0.0495	1940	0.29	8.6×10^{16}	19.9
0.07	1940	0.29	1.07×10^{17}	20.2

^aRepresentative case presented in Fig. 2.

with a homogeneous plasma rather than the steplike density, the differences in the pulse duration and intensity after the same propagation distance were only 6% and 10%, respectively.

Finally, we investigate the effects of pump length on the pulse compression. When the pump length was reduced by half from the case of Fig. 2, preserving the total pump energy $\propto a_2^2 \tau_2$ constant (the second line in Table I), the seed pulse was shortened even more (up to 14 fs). The intensity gain of the seed decreased, since the electron trapping enhanced by the intensified pump prevented efficient energy transfer from the pump to the seed.¹⁰ When the pump length was prolonged by a factor of 2 from the case of Fig. 2 (the fourth and fifth rows in Table I), the intensity gains of the seed were higher than that in Fig. 2. However, the final pulse durations of the seed are much longer than the short pump cases, which are contradictory to the general expectation. Figure 4(a) represents the temporal evolution of the FWHM of the seed pulse for the last case in Table I. In the early stage, the pulse duration decreases as time goes on, but begins to increase again after some time. The snapshots of the pulse shape in Fig. 4(b) show that as time advances, the front half of the pulse is blown up, while the rear half remains almost unchanged, leading to the increase of the pulse duration. The different pulse evolutions in the front and rear parts indicate

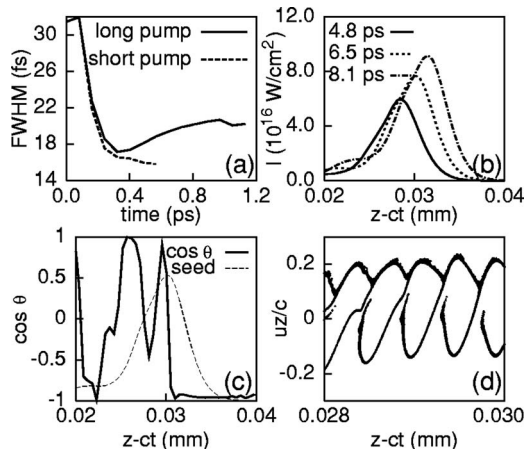


FIG. 4. (a) Evolution of the seed pulse duration. The long pump result corresponds to the last case in Table I. The short pump case is from Fig. 2. (b) The snapshots of the seed pulse for the long pump case in (a). (c) Cosine of the relative phase between the seed, pump, and plasma waves, measured at $t=6.5$ ps. The dashed line is the corresponding seed profile. (d) The phase space of the electron plasma just behind the peak of the seed in (c).

that the energy exchange between the waves and the plasma in the rear part is negligible compared to that in the front part. The origin of such behavior could be illuminated by measuring the relative phase between the three waves $\theta \equiv \theta_1 - \theta_2 + \theta_p$, where the seed and pump phases are defined by $\theta_{1,2} = \arctan[\text{Im } a_{1,2} / \text{Re } a_{1,2}]$, respectively. In the same way, the phase θ_p of the plasma wave is calculated from the plasma wave envelope f defined by Eq. (1c). From the consideration that the energy flow from the pump to the seed is proportional to $-\cos \theta$,¹⁰ it is seen in Fig. 4(c) that the front half of the pulse keeps getting energy from pump ($-\cos \theta \sim 1$). Behind the peak, however, the energy exchange between the waves is not so fluent as in the front half, since the strong wave breaking [Fig. 4(d)] of the plasma wave induces a relatively fast oscillation of the sign of $-\cos \theta$.¹⁰ Note that for all the simulations listed in Table I, the electrons near the output edge of the plasma slab experience less than a single temporal oscillation, i.e., $\tau_1 \omega_p / 2\pi < 20 \text{ fs} \times 0.047 \text{ fs}^{-1} \sim 1$, where τ_1 is the seed pulse duration.

In summary, we performed the kinetic simulations of laser pulse compression by the RBS scheme in the super-radiant regime. The most interesting aspect of our work is that we investigated the regime of extremely short interaction of the seed pulse with intense Gaussian pump pulses, which has not been studied before. In the representative case, a 31 fs seed pulse was compressed to 15.8 fs, $7.3 \times 10^{16} \text{ W/cm}^2$, by using the pump pulse of 970 fs and $8.2 \times 10^{15} \text{ W/cm}^2$. When a reasonable value for the spot size is assumed, this corresponds to a laser beam of tens of terawatts. The required plasma size is just 0.145 mm in the laser propagation direction and 0.8 mm in the transverse direction, whose uniformity and fluctuation can be put under control more easily than the millimeter-order long plasmas. It was found that the rate of amplification and pulse shortening is quite robust to the variation in the initial delay between the seed and pump pulses. It was shown by the analysis of the relative phase that the pulse duration increases by the long interaction, which is a contradictory result to the previous expectations.

This work was financially supported by the Creative Research Initiatives Program/KOSEF of the Korea Ministry of Science and Technology.

- ¹W. P. Leemans, B. Nagler, A. J. Gonsalves, Cs. Toth, K. Nakamura, C. G. R. Geddes, E. Esarey, C. B. Schroeder, and S. M. Hooker, *Nat. Phys.* **2**, 696 (2006).
- ²J. Lindl, *Phys. Plasmas* **2**, 3933 (1995).
- ³G. Cerullo, M. Nisoli, S. Stagira, and S. De Silvestri, *Opt. Lett.* **23**, 1283 (1998).
- ⁴A. Shirakawa, I. Sakane, and T. Kobayashi, *Opt. Lett.* **23**, 1292 (1998).
- ⁵V. M. Malkin, G. Shvets, and N. J. Fisch, *Phys. Rev. Lett.* **82**, 4448 (1999).
- ⁶M. S. Hur, G. Penn, J. S. Wurtele, and R. R. Lindberg, *Phys. Plasmas* **11**, 5204 (2004).
- ⁷M. Dreher, E. Takahashi, J. Meyer-ter-Vehn, and K.-J. Witte, *Phys. Rev. Lett.* **93**, 095001 (2004).
- ⁸W. Cheng, Y. Avitzour, Y. Ping, S. Suckewer, N. J. Fisch, M. S. Hur, and J. S. Wurtele, *Phys. Rev. Lett.* **94**, 045003 (2005).
- ⁹G. Shvets, N. J. Fisch, A. Pukhov, and J. Meyer-ter-Vehn, *Phys. Rev. Lett.* **81**, 4879 (1998).
- ¹⁰M. S. Hur, R. R. Lindberg, A. E. Charman, J. S. Wurtele, and H. Suk, *Phys. Rev. Lett.* **95**, 115003 (2005).